Neuro-Oncology
19(4), 493–502, 2017 | doi:10.1093/neuonc/now179 | Advance Access date 23 September 2016

Immunovirotherapy with measles virus strains in combination with anti–PD-1 antibody blockade enhances antitumor activity in glioblastoma treatment

Jayson Hardcastle,* Lisa Mills,* Courtney S. Malo, Fang Jin, Cheyne Kurokawa, Hirosha Geekiyanage, Mark Schroeder, Jann Sarkaria, Aaron J. Johnson, Evanthia Galanis

Department of Molecular Medicine, Mayo Clinic, Rochester, Minnesota (J.H., L.M., C.K., H.G., E.G.); Department of Immunology, Mayo Clinic, Rochester, Minnesota (C.S.M., F.J., A.J.J.); Mayo Clinic Graduate School, Mayo Clinic, Rochester, Minnesota (C.K.); Department of Radiation Oncology, Mayo Clinic, Rochester, Minnesota (M.S., J.S.); Department of Neurology Mayo Clinic, Rochester, Minnesota (A.J.J.); Oncology, Division of Medical Oncology, Mayo Clinic, Rochester, Minnesota (J.H., H.G., E.G.)

Corresponding Author: Evanthia Galanis, MD, Mayo Clinic, 200 First Street SW, Rochester, MN 55905 (galanis.evanthia@mayo.edu).

*J.H. and L.M. contributed equally.

Abstract

Background. Glioblastoma (GBM) is the most common primary malignant brain tumor and has a dismal prognosis. Measles virus (MV) therapy of GBM is a promising strategy due to preclinical efficacy, excellent clinical safety, and its ability to evoke antitumor pro-inflammatory responses. We hypothesized that combining anti– programmed cell death protein 1 (anti-PD-1) blockade and MV therapy can overcome immunosuppression and enhance immune effector cell responses against GBM, thus improving therapeutic outcome.

Methods. *In vitro* assays of MV infection of glioma cells and infected glioma cells with mouse microglia ± aPD-1 blockade were established to assess damage associated molecular pattern (DAMP) molecule production, migration, and pro-inflammatory effects. C57BL/6 or athymic mice bearing syngeneic orthotopic GL261 gliomas were treated with MV, aPD-1, and combination treatment. T2* weighted immune cell-specific MRI and fluorescence activated cell sorting (FACS) analysis of treated mouse brains was used to examine adaptive immune responses following therapy.

Results. *In vitro*, MV infection induced human GBM cell secretion of DAMP (high-mobility group protein 1, heat shock protein 90) and upregulated programmed cell death ligand 1 (PD-L1). MV infection of GL261 murine glioma cells resulted in a pro-inflammatory response and increased migration of BV2 microglia. In vivo, MV + aPD-1 therapy synergistically enhanced survival of C57BL/6 mice bearing syngeneic orthotopic GL261 gliomas. MRI showed increased inflammatory cell influx into the brains of mice treated with MV+aPD-1; FACS analysis confirmed increased T-cell influx predominantly consisting of activated CD8 +T cells.

Conclusions. This report demonstrates that oncolytic measles virotherapy in combination with aPD-1 blockade significantly improves survival outcome in a syngeneic GBM model and supports the potential of clinical/translational strategies combining MV with αPD-1 therapy in GBM treatment.

Key words

aPD-1 | glioblastoma | immunovirotherapy | measles virus

Glioblastoma (GBM) is the most common primary malignant brain tumor in adults. Despite aggressive multimodality therapy, median survival is dismal at 15–16 months from diagnosis,[1] with an urgent need for novel therapeutic approaches. We have previously demonstrated the efficacy of measles virus (MV) strains derived from the

Edmonston vaccine (MV-Edm) lineage, including derivatives engineered to express the human carcinoembryonic antigen (MV-CEA) and the sodium-iodide symporter gene (MV-NIS) against orthotopic primary patient derived GBM xenografts.[2–6] In addition, we have retargeted MV against GBM by redirecting viral entry via epidermal growth factor receptor (EGFR) (MV-EGFR),[7] EGFVR variant III (MV-EGFRvIII),[4] and interleukin (IL)-13Rα2[3] receptor, thus increasing the specificity of MV infection. These results were translated into an ongoing phase I clinical trial for recurrent GBM patients.

MV is a single-stranded, negative-sense, enveloped RNA paramyxovirus. The viral genome has 6 genes encoding 8 proteins.[8] The MV hemagglutinin protein mediates viral attachment to its 3 known receptors, CD46,[9] signaling lymphocytic activation molecule (SLAM),[10] and nectin-4.[11] Wild-type MV primarily enters cells through the SLAM receptor, whereas the serially passaged MV-Edm vaccine strains primarily enter cells through the CD46 receptor[8,11]; CD46 is ubiquitously expressed on nucleated primate cells and overexpressed in tumors, including GBM.[8] The third MV receptor, nectin-4, is expressed in the respiratory epithelium[11] but also in ovarian, breast, and lung cancers,[12–14] as well as GBM.[15] Overexpression of MV receptors in human cancers allows for preferential attachment, entry, and selectivity of MV-Edm strains for cancer therapy.

GBM tumors are highly immunosuppressive, including increased levels of programmed cell death ligand 1 (PD-L1) expression,[16,17] regulatory T cells (T_{regs}), accumulation[18] monocyte co-option,[19] PD-L1 upregulation on tumor associated macrophage,[17,19] and systemic immune suppression[20]; resulting in tumor growth and immune evasion. Cancer therapy with functional blocking antibodies against programmed cell death protein 1 (PD-1) or PD-L1 can restore effector T-cell proliferation and antitumor activity. Two different anti–PD-1 (aPD-1) antibodies—nivolumab (Opdivo) and pembrolizumab (Keytruda)—have been FDA approved for the treatment of melanoma, lung cancer, and renal cell carcinoma. Clinical trials with aPD-1 or anti–PD-L1 antibodies in newly diagnosed or recurrent GBM are ongoing or nearing completion.

Oncolytic viral (OV) infection of tumor cells can initiate antitumor immune responses from the production of pathogen associated chemokines and cytokines, and release of damage-associated molecular pattern (DAMP)[21–26] molecules and tumor-associated antigens.[27] Supporting the above, in a recently reported clinical trial of measles virotherapy in ovarian cancer, MV therapy was associated with prolongation of survival and induced a type 1 T helper cell (Th1) immune response against tumor-specific antigens, suggesting that the antitumor effect was in part immune mediated.[28]

We therefore hypothesized that MV therapy in combination with aPD-1 checkpoint inhibition could significantly complement each other's activity in GBM treatment. Herein we show that MV infection of primary patient GBM cells results in *in vitro* production and release of DAMPs such as high-mobility group protein 1 (HMGB1) and heat shock protein 90 (HSP90), potentially setting the stage for a pro-inflammatory response in vivo. Upon treatment of mice bearing orthotopic GL261 gliomas with MV-EGFR+aPD-1, there was significant prolongation of survival compared with single-agent therapy, a benefit lost in athymic mice. Mice treated with MV-EGFR+aPD-1 had increased CD8+ T-cell influx into their brains by MRI and fluorescence activated cell sorting (FACS) analysis. Collectively these data can have significant translational implications in GBM treatment.

Materials and Methods

Cell Culture

GL261 murine glioma cells, murine BV2 microglia cells (BV2) (a gift from the Godbout Lab, The Ohio State University), were grown in Dulbecco's modified Eagle's medium (DMEM) containing 10% fetal bovine serum with Pen-Strep (10F DMEM). Primary patient derived glioblastoma lines GBM39, GBM12, GBM10, GBM76, and GBM14 were generated from glioblastoma patients under a Mayo Clinic institutional review board approved protocol and maintained as subcutaneous xenografts and short-term *in vitro* cultures as previously described.[29]

Viruses

MV-EGFR, MV-EGFRvIII, MV-NIS, and MV–green fluorescent protein (GFP) were constructed as previously described.[4,7,30,31]

Assessment of MV Titers

This was performed as previously described[2] (see Supplementary material).

Programmed Cell Death Ligand 1, Human Leukocyte Antigen–ABC, and Human Leukocyte Antigen–G Fluorescence Activated Cell Sorting

Cells were plated in 6-well dishes (5×10^5 cells/well) in 10F media. The following day, species-respective interferon (IFN)-γ (500U/mL; eBioscience #14-8319-80 or #14-8311-63) was added ($n = 3$ wells per cell line) or cells were infected with MV-EGFR (multiplicity of infection [MOI] = 1), MV-NIS, or ultraviolet (UV)-inactivated MV-EGFR or MV-NIS. FACS analysis was performed 24 and 36 hours later for the indicated markers (see Supplementary material and Supplementary Table 1).

Coculture Assays for Quantitative Real-Time PCR

GL261 cells were plated (7.5×10^5/well) in 2F DMEM and infected with MV-EGFR (MOI = 3) or left uninfected. Coculture assays were then performed with BV2 cells as previously reported.[32] Human cocultures were treated with aPD-1 (1 μg/mL; eBioscience #16-9989-38) or immunoglobulin (Ig)G1-κ (20 μg/mL; Sigma #15154-1146) or left untreated ($n = 2$ wells/group). RNA was isolated, cDNA synthesis performed, and quantitative real-time (qRT)-PCR conducted using the primers indicated (Supplementary Table 2).

Western Blot for High-Mobility Group Protein 1 and Heat Shock Protein 90

GBM39 and GBM12 cells were plated (2.5×10^5 cells) in 1F DMEM, and infected with UV light inactivated MV-NIS (UV-MV-NIS) or MV-NIS (MOI = 0.5) or left untreated. At time points indicated, cell medium (CM) was removed and the cells lysed in Triton lysis buffer. Equal amounts were run for western blot, and proteins of interest were probed for, as previously described.[22] Western blot antibodies used are detailed in the Supplementary material.

Transwell Assays

Transwell assays were performed using MV infected GL261 cells. BV2 cells were harvested and added to the transwell inserts. aPD-1 (1 μg/mL), IgG1-κ (20 μg/mL), and concentrated conditioned CM (derived from infected and uninfected respective cells and concentrated in Millipore [centrifuge filters #UFC90324]) was added. Inserts were then stained with 4′,6′-diamidino-2-phenylindole, and the average number of migrated monocytes enumerated. Additional information is provided in the Supplementary material.

Animal Experiments

All animal experiments were approved by the Mayo Institutional Animal Care and Use Committee. Orthotopic tumors were established by implantation of 3×10^5 GL261 cells,[2–6] into the caudate nucleus, using a small animal stereotactic frame (ASI Instruments) and a 26-gauge Hamilton syringe. Athymic nu/nu mice were obtained from Harlan and C57BL/6 mice from Charles River Laboratories. MV-EGFR or UV-MV-EGFR was administered at 2×10^5 per median tissue culture infectious dose ($TCID_{50}$) intratumorally using the same coordinates as for cell implantation. Murine aPD-1 (200 μg/mouse) (BioLegend #114110) was administered i.p.

Ex vivo Fluorescence Activated Cell Sorting Analysis

Mice were treated as previously described under "Animal Experiments." On day 11 post tumor implantation, mice were euthanized, their brains removed, cerebellums discarded, and lymphocytes isolated from the rest of the brain. The list of fluorochrome conjugated antibodies used in FACS analysis is provided in the Supplementary material.

MRI for Detection of Inflammatory Cells and T Cells

All MR imaging was performed on a Bruker Ultrashield 300 MHz (7T) vertical bore nuclear MR spectrometer equipped with "mini-imaging" accessories as previously described.[33]

Detection of Tumor Monocytic Infiltration by MRI

GL261 tumor cells were implanted orthotopically into C57BL/6 mice as described in "Animal Experiments." Seven days later, the mice were injected with MV-EGFR or UV-MV-EGFR (2×10^5 $TCID_{50}$, 10μL) or were left untreated. In order to visualize inflammatory cells, mice received tail vein injections of 100 μL of FeraSpin particles (Miltenyi #130-095-171) and underwent T2 MRI (spoiled gradient echo: 7ms, rep: 50ms, excitation [length: 1ms, flip angle: 40degrees, atten: 12.7 dB]) daily for 3 days following MV therapy.

Detection of T Cells by MRI

In a separate experiment, mice bearing syngeneic orthotopic GL261 glioma xenografts were treated as described under "Animal Experiments." On day 10 post tumor implantation, all mice received labeled CD4 (#130-049-201) and CD8a (#130-049-401) microbeads (Miltenyi) via tail vein as previously described.[33] The following day, the mice underwent T2* MRI (spoiled gradient echo: 2ms, rep: 26.405ms, excitation [length: 1ms, flip angle: 30degrees, atten: 20.1 dB]).

All scans were analyzed with Analyze 12.0 software and positive areas in the brains enumerated and shown as average monocrystalline iron oxide nanoparticle (MION) contrast agent volume/brain. For T-cell MRI analysis, MION volume/brain was subtracted from the MION-positive area of untreated brains to yield the shown average MION volume/mouse brain.

Statistical Analysis

Kaplan–Meier survival curves were used to assess animal survival, and comparisons were performed using the log-rank test. ANOVA with a post-hoc Tukey test was employed to analyze FACS and MRI data. All other assays used Student's *t*-test for analysis. $P < .05$ was considered statistically significant.

Results

Variable Upregulation of Programmed Cell Death Ligand 1 and Human Leukocyte Antigen–ABC upon Interferon-γ Stimulation of GBM Cells

MV infection has been shown to elicit an immune mediated IFN-γ response.[34] Previous reports have shown that IFN-γ stimulation of tumor cells can result in increased expression of immunomodulatory molecules such as PD-L1, human leukocyte antigen (HLA)–ABC, and/or HLA-G. We therefore examined the expression changes of these molecules in primary patient derived GBM lines and murine GBM lines following IFN-γ treatment. We demonstrated that PD-L1 expression is upregulated in the human GBM cell lines GBM 39 and GBM12 at 24 and 36 hours post IFN-γ treatment (Fig. 1A–1D). Additionally, the murine GL261 glioma cell line constitutively expressed high levels of PD-L1, which was only modestly increased following IFN-γ treatment (Fig. 1E–1F). IFN-γ treatment had a variable impact on expression of HLA-ABC molecules, with upregulation being observed in 2 of 5 primary GBM lines

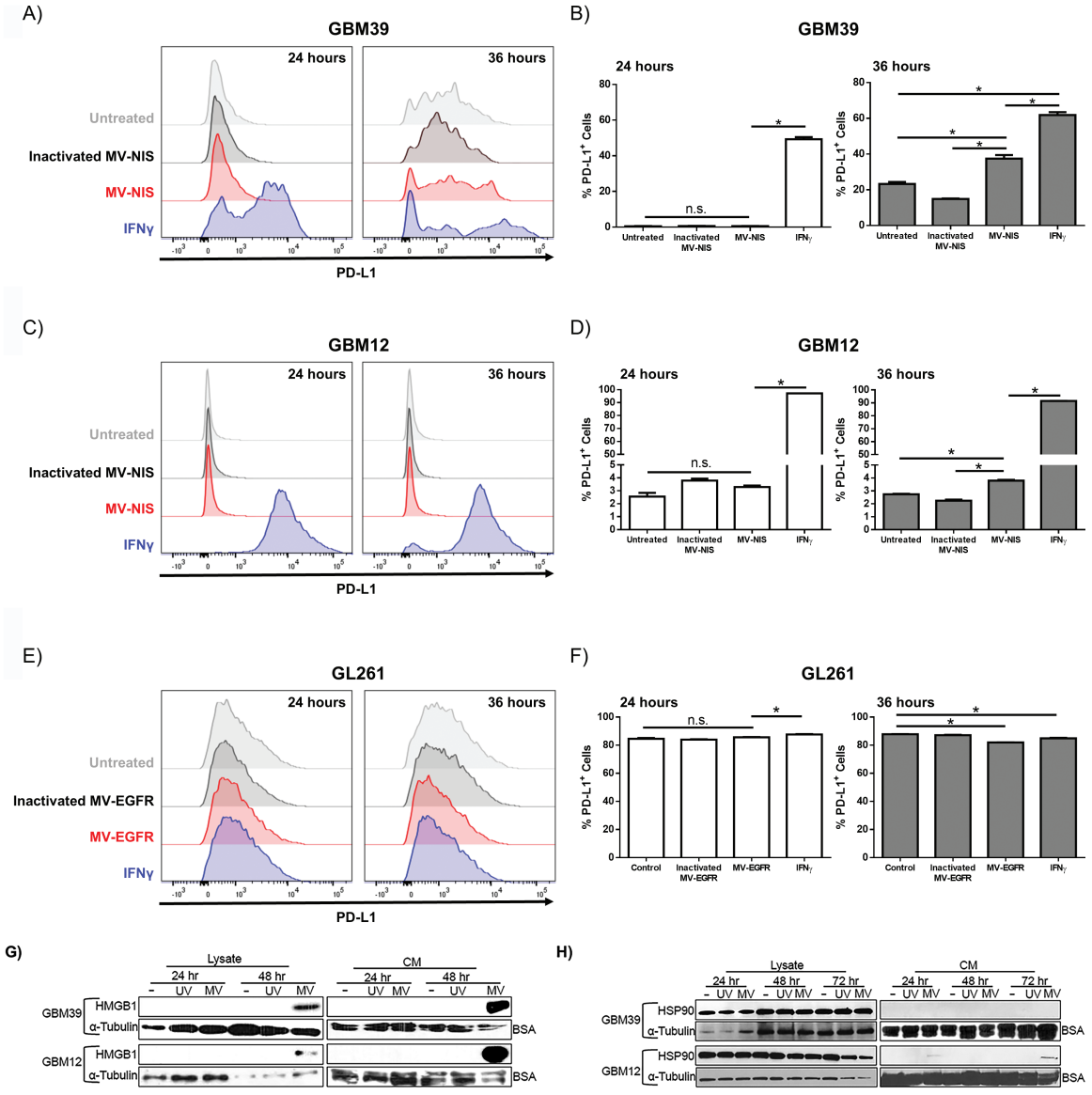

Fig. 1 In vitro IFN-γ treatment or MV infection of GBM cells modulates expression of PD-L1. Human GBM39 (A–B), GBM12 (C–D), or murine GL261 (E–F) were treated with MV, inactivated MV, or IFN-γ and assessed for PD-L1 expression by flow cytometry 24 and 36 hours post treatment ($N = 2$ per treatment). (A, C) Representative flow cytometry histograms and (B, D) quantification of PD-L1 expression demonstrate that IFN-γ increases PD-L1 expression on GBM39 cells and GBM12 cells. (E) Representative histograms and (F) quantification demonstrate that the GL261 glioma cell line expresses high levels of PD-L1 independent of treatment. Error bars represent mean±SEM. * denotes $P<.05$. Expression of HMBG1 and HSP90 by western immunoblotting in untreated (-), UV-MV-NIS (UV), and MV-NIS treated GBM39 and GBM12 cells at the indicated time points post-infection: increased expression of HMGB1 was detected both in lysates and CM at 48 hours (G); increased expression of HSP90 was only detected in CM of GBM12 cells (H).

tested (Supplementary Fig. 1 and Supplementary Table 1). Upregulation of the immune inhibitory molecule HLA-G was observed in only 1 of 5 primary GBM lines.

Early MV Infection of GBM Cells Upregulates Molecules Involved in Immune Evasion Pathways

We next assessed the effect that MV infection of GBM cells has on PD-L1 expression *in vitro*. Human GBM cells were infected with MV-NIS, an oncolytic MV strain currently in clinical testing. UV-inactivated MV-NIS treated cells and untreated cells were used as controls. Murine GL261 cells are not infectable with MV-NIS due to lack of expression of natural MV receptors in rodent lines, and thus they were infected with the retargeted strain MV-EGFR. Analysis by flow cytometry following 24- and 36-hour incubation showed that MV-NIS infection increased PD-L1 expression on both human cell lines by 36 hours (Fig. 1A–1D). GL261

cells continued to express high levels of PD-L1 regardless of treatment (Fig. 1E–1F). Consistent with the IFN-γ treatment results, we observed only modest differences in major histocompatibility complex I expression (human HLA-ABC or murine H2-K^b) in MV infected cells (Supplementary Fig. 1). Likewise, we saw minimal differences in human HLA-G or murine Qa-2 expression (Supplementary Fig. 1). Together, these data indicate that the inflammatory environment mediated by MV infection promotes PD-L1 expression in human GBM. Additionally, high expression of PD-L1 by the GL261 glioma cell line suggests that aPD-1 could have therapeutic utility in combination with MV therapy.

MV Infection of Human GBM Cells Can Result in High-Mobility Group Protein 1 and Heat Shock Protein 90 Production

Oncolytic virus infection of tumor cells has been shown to result in the production of DAMPs, including HMGB1 and HSP90, which can augment an immune response.[21–26,35] We therefore examined MV infected primary patient GBM12 and GBM39 lines for DAMP production. CM and cell lysate from treated cells were probed by western immunoblotting for the indicated proteins (Fig. 1G, 1H). MV infection resulted in a significant increase in the production of the pro-inflammatory mediator HMGB1 at 48 hours post MV infection in both primary GBM cell lines (Fig. 1G). Increased production of secreted HSP90 was also observed following infection of primary GBM12, but not GBM39 cells (Fig. 1H).

Murine GL261 Glioma Cells Can Be Infected by MV-EGFR but Infection Is Nonproductive

The assessment of MV+aPD-1 activity in vivo required testing in an immunocompetent syngeneic murine model. Murine cells do not express the natural MV receptors CD46, nectin-4, or SLAM to allow for MV infection.[36,37] To circumvent this barrier, we used retargeted MV that infects murine cells via alternative receptors. Prior to initiation of in vivo studies, we sought to determine whether GL261 glioma cells were infectable by retargeted MV strains. Briefly, the EGFR-expressing[38] GL261 cells were infected with MV-GFP, MV-EGFR, MV-EGFRvIII (MOI = 3) or UV-inactivated MV strains. The MV-EGFR and MV-EGFRvIII strains also encode GFP. Following infection, MV-produced GFP expression was assessed by FACS (Fig. 2A) and fluorescent microscopy (Fig. 2B) to confirm infection. Vero cells infected with MV-GFP (MOI = 1) for 24 hours were used as a positive control. Results showed GFP production in GL261 cells infected at low levels by MV-EGFR. These results were confirmed and quantified by FACS, showing that an MOI = 3 yields approximately 15% infection.

MV-EGFR Infection of Murine GL261 Glioma Cells Significantly Increases Pro-Inflammatory and Pro-Migratory Responses of BV2

Microglia are resident monocytes of the central nervous system.[39] BV2 microglia are immortalized microglia isolated from C57BL/6 mice and represent an alternative model system to primary microglia.[40,41] Using BV2, we analyzed the effects of MV-EGFR infection of murine GL261 GBM cells (Fig. 2C) in coculture. Quantitative RT-PCR for pro-inflammatory gene expression showed significant increase in mRNA levels for IFN-α, IFN-β, and IFN-γ in cocultures of BV2+MV-EGFR+GL261 cells compared with uninfected cocultures ($P<.05$; Fig. 2C). These results indicate that MV-EGFR infection of GL261 cells is capable of stimulating a pro-inflammatory response in murine microglia.

Transwell assays were used to assess whether MV-EGFR infection of GL261 cells could increase BV2 migratory response. MV infection of GL261 cells significantly increased the pro-migratory response of BV2 microglia compared with uninfected GL261 cells ($P = .039$; Fig. 2D).

MV-EGFR Therapy of Mice Bearing Orthotopic GL261 Gliomas Elicits a Pro-Inflammatory Response as Assessed by Monocyte MION MRI Analysis

We next sought to determine whether MV-EGFR therapy of mice bearing syngeneic orthotopic GL261 gliomas elicits a pro-inflammatory response. For this we employed monocyte MRI analysis using MION as previously described.[42] Seven days post tumor implantation the mice received a single intratumoral dose of UV-MV-EGR or MV-EGFR (2×10^5TCID$_{50}$) or were left untreated ($n = 3$/group). T2 weighted MRI obtained at 24 hours post MV therapy (Fig. 2E) showed increased influx of monocytes into the brains of mice treated with MV-EGFR compared with the other therapy groups. Figure 2F is a representative reconstruction of day 1 MRI (red shading = MION positive areas). These results combined with the results of the BV2 assays indicate that treatment of GL261 gliomas with MV-EGFR results in a monocyte inflammatory response in vivo; this inflammatory response sharply decreases after day 1 in vivo, possibly as a result of the limited ability of the MV-EGFR virus to replicate in murine lines, including GL261.

MV-EGFR Therapy in Combination with aPD-1 Blockade Therapy Significantly Enhances Survival of Mice Bearing Syngeneic Orthotopic GL261 Gliomas

Following *in vitro* evidence of MV-EGFR infection of GL261, we employed the orthotopic GL261 tumor model in order to assess the in vivo efficacy of MV+aPD-1 therapy. C57BL/6 mice bearing orthotopic GL261 gliomas were treated as outlined in "Materials and Methods" following the timeline shown in Fig. 3A. Mice which received MV-EGFR+aPD-1 had a significant enhancement of survival compared with the other therapy groups (vs untreated [$P = .0039$], vs MV-EGFR [$P = .0097$], vs aPD-1 [$P = .0387$]) (Fig. 3A). Sixty percent of the mice were deemed long-term survivors, remaining alive for at least 120 days.

Mice that received the aPD-1 monotherapy regimen had significant survival enhancement compared with untreated mice ($P = .0039$) but not compared with MV-EGFR therapy regimen treated mice ($P = .0636$). There was no

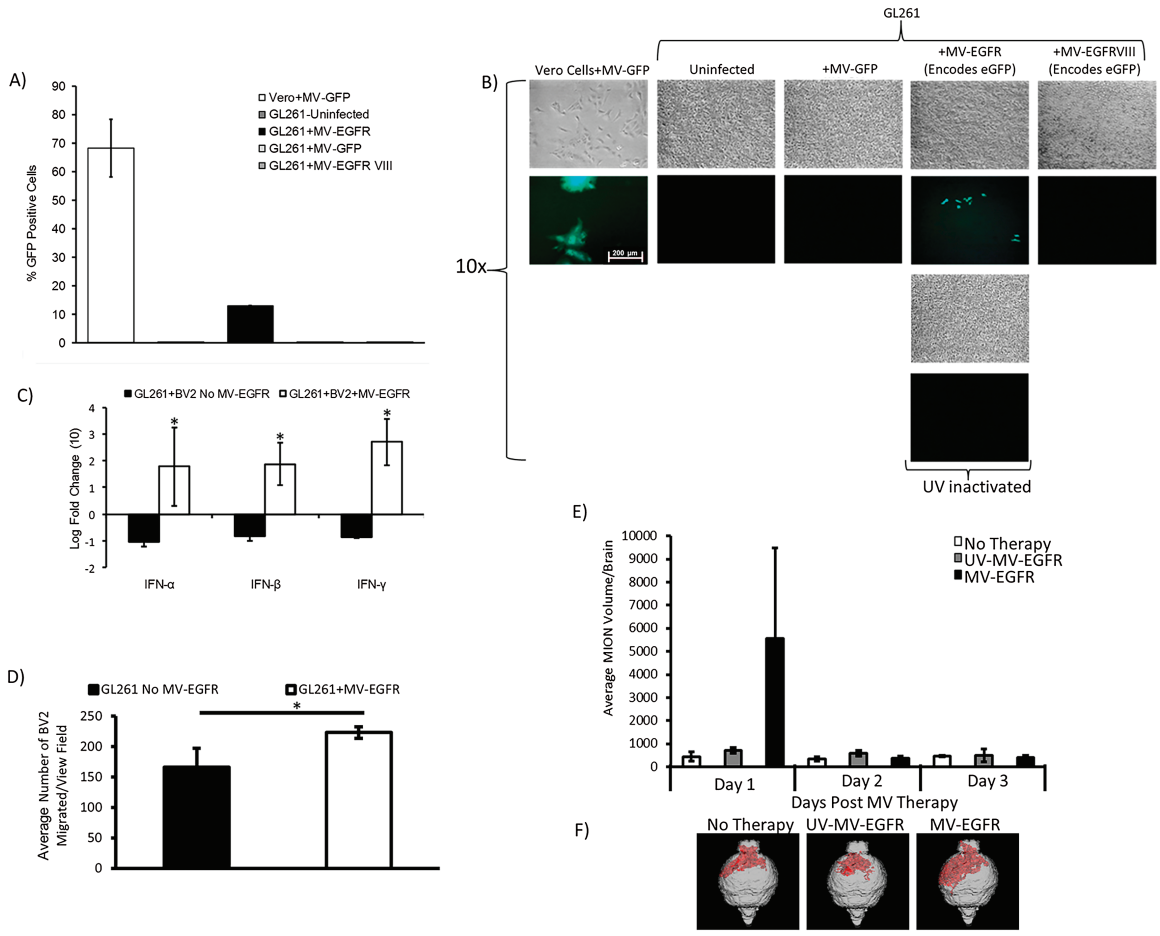

Fig. 2 MV-EGFR infection of murine GL261 glioma cells is limited, but stimulates pro-inflammatory responses *in vitro* and in vivo. (A) GFP FACS quantification in MV infected GL261 cells. (B) GFP detection by fluorescence microscopy pictures 3 days post infection of GL261 with MV or corresponding UV inactivated constructs (MOI = 3, scale bar = 200 µm). (C) Results of qRT-PCR of BV2 cocultures with MV-EGFR infected GL261 cells. IFN-α, IFN-β, and IFN-γ were significantly upregulated compared with uninfected GL261 cells (**P*<.05). (D) MV-EGFR infection of GL261 cells significantly increased BV2 transwell migration (**P*<.05) (E) Average MION volume from T2 weighted MRI of orthotopic GL261 tumors treated with MV-EGFR, UV-MV-EGFR, or untreated (n = 3/group). Increased MION volume (monocytic infiltration) into the brains of MV-EGFR treated mice was observed one day post therapy. (F) Representative MION MRI reconstructions (red shading = MION+).

significant enhancement of survival for mice treated with the MV-EGFR therapy regimen alone compared with untreated mice (P = .1283). Treatment with aPD-1 was well tolerated in this model, with no systemic or neurologic toxicity being observed.

MV-EGFR+aPD-1 Therapy of Mice Bearing Syngeneic Orthotopic GL261 Glioma Increases Tumor T-Cell Influx as Assessed by T2* MRI

Next we sought to determine whether the significantly enhanced survival observed in the MV-EGFR+aPD-1 group was due to an immune effect. In a parallel experiment using the same GL261 efficacy model, mice were treated as shown in the Fig. 3B timeline. Mice received a tail vein injection of CD4 and CD8 antibody conjugated ultrasmall superparamagnetic iron oxide particles (USPIO) using a previously established protocol[33]; quantification of the USPIO-positive area from T2* MRI on day 11 post tumor implantation showed that mice receiving MV-EGFR+aPD-1 had a larger influx of T cells into their brains compared with all other therapy groups. Representative reconstructions of scans shown (Fig. 3C) visually illustrate this effect. These T2* MRI results support a T-cell mediated immune response in the MV-EGFR+aPD-1 therapy treated group.

Mice Bearing Orthotopic GL261 Tumors Treated with MV-EGFR+aPD1 Have an Increased Influx of Granzyme B+ CD8+ T Cells

In a separate experiment, C57BL/6 mice bearing GL261 orthotopic tumors were treated according to the Fig. 3A timeline. Lymphocytes isolated from the brain of GL261 bearing mice were analyzed via flow cytometry at 11 days

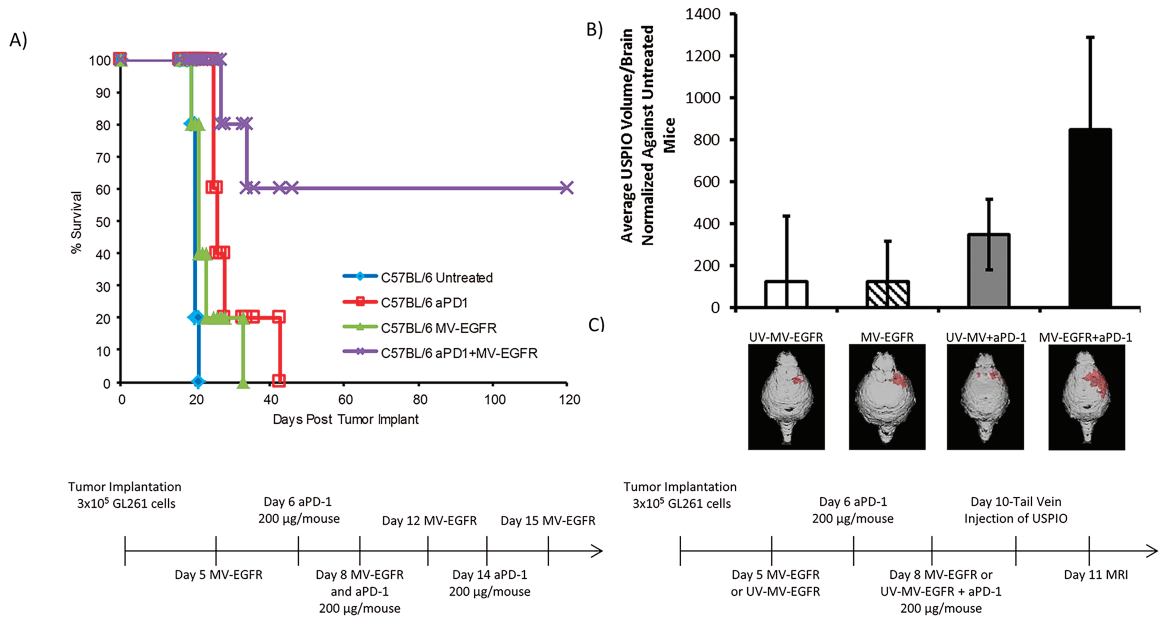

Fig. 3 MV-EGFR+aPD-1 therapy significantly enhanced survival of mice bearing orthotopic GL261 gliomas and increased T cell influx into their brains as assessed by T2* MRI. (A) Kaplan–Meier survival curves of mice bearing orthotopic GL261 gliomas treated as indicated. MV-EGFR+aPD-1 treatment resulted in significant enhancement of survival compared with all other groups. aPD-1 therapy resulted in significant enhancement of survival compared with untreated mice but not compared with MV-EGFR treated mice. (B) T2* MRI analysis of T-cell influx into mouse brains on day 11 post tumor implantation. MV-EGFR+aPD-1 therapy group had increased T-cell influx compared with other groups. (C) Representative T2* MRI reconstructions (red shading = USPIO positive).

post tumor implantation, the same time point assessed via T2* MRI in Fig. 3. Flow cytometry analysis demonstrated increased influx of T cells (CD3+ CD45.2hi) into the brains of mice treated with MV-EGFR+aPD-1 (Fig. 4A, 4B). Further characterization of the T-cell subpopulations revealed that mice treated with MV-EGFR+aPD-1 had a higher percentage of CD8+ T cells (Fig. 4C), an increased percentage of CD8+GzmB+ T cells (Fig. 4D), as well as an increase in the CD8+ T cell:T_{reg} ratio (Fig. 4E) compared with no treatment, treatment with UV-inactivated virus, or monotherapy. Examination of total CD4+ T cells, as well as the T_{reg} (CD3+ CD45.2hi+ FoxP3+) or conventional T cell (CD3 +CD445.2hi CD4+ FoxP3–) subpopulations demonstrated no significant difference between treatment groups (data not shown).

Enhanced Survival Observed with MV-EGFR+aPD-1 Is Dependent on T-Cell Mediated Responses

To further investigate whether a T-cell mediated response is required for the observed enhanced survival in the MV-EGFR+aPD-1 therapy group (Fig. 3A), we established GL261 gliomas by implanting 3 × 10^5 cells orthotopically in the caudate nucleus of athymic nude mice. The mice received the same therapy regimen that was used in the GL261, C57BL/6 model (n = 5/group). Survival analysis showed loss of survival enhancement for the MV-EGFR+aPD-1 treatment group compared with untreated mice (P = .2143) (Fig. 5). Furthermore, there was no difference in survival between untreated and aPD-1 treated mice (P = .1311). This supports the requirement of a T-cell mediated response for the observed increase in survival for both the aPD-1 and the MV-EGFR+aPD-1 combination therapy in the C57BL/6 GL261 orthotopic model.

Discussion

In this manuscript we demonstrate for the first time that oncolytic (MV platform based) virotherapy has synergistic activity with aPD-1 therapy in GBM treatment. These data complement previous reports in B16 melanoma, using Reovirus,[43] or MV engineered to express anti-CTLA4 or anti–PD-L1 antibodies.[44]

Oncolytic virotherapy of cancer has shown preclinical promise and it is currently being clinically evaluated in GBM treatment.[45,46] OV infection of tumor cells has also been shown to initiate systemic antitumor/antiviral immune responses.[22,23,25,26,35] There is accumulating evidence that MV infection has immunostimulatory properties. Donnelly and colleagues showed that MV infection of human melanoma cell lines induced a dose-dependent increase in IL-6 and IL-8, as well as variable increase in IFN-α, IFN-β, and IFN-λ.[22] Moreover, MV infection in melanoma led to dendritic cell activation stimulating a CD8+ cytotoxic T-cell response. In clinical trials, MV treatment of ovarian

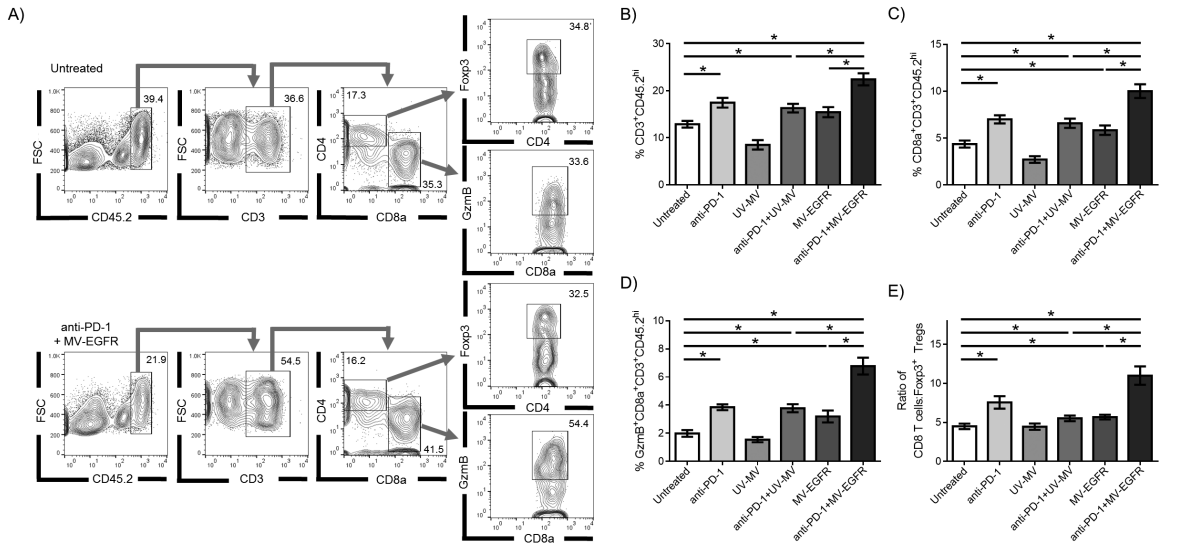

Fig. 4 MV-EGFR+aPD-1 treatment enhances CD8 T-cell influx into the brain of GL261-bearing animals. Brains isolated from treated GL261-bearing animals were assessed for immune cell infiltration (N = 9 per group) (A) Representative flow cytometry histograms depicting gating scheme. (B) An increased proportion of T cells (CD3+CD45.2^{hi}) were isolated from animals treated with combination therapy compared with monotherapy. (C) A higher proportion of CD8 T cells (CD8α+CD3+CD45.2hi) were isolated from the brains of dually treated animals, and (D) more of those cells were positive for granzyme B (GzmB+). (E) An increase in the CD8 T cell:Foxp3+ Treg ratio in the brain was also observed in MV-EGFR+aPD-1 treated animals. Error bars represent mean±SEM. * denotes P<.05.

cancer patients generated a tumor-specific Th1 response.[28] Findings presented in this manuscript support the immunostimulatory potential of MV infection against GBM.

GBM tumors are immunosuppressive,[17,19,47] and reversal of this status—for example, by using immune checkpoint blockade—could lead to improvement in outcome. A number of clinical trials for newly diagnosed or recurrent GBM patients using aPD-1 or anti–PDL-1 antibodies are currently ongoing or soon to be activated, while combinatorial strategies are also evolving. In this manuscript, we showed that combined oncolytic MV therapy and aPD-1 therapy significantly increases antitumor activity in immunocompetent mice compared with single-agent aPD-1 treatment. In *in vitro* work, we demonstrated that MV infection of GBM lines resulted in an initial increase of the immune evasion molecule PD-L1, supporting the rationale of a combinatorial strategy with aPD-1 or PD-L1 blockade. As the MV infection progresses, infected GBM cells produce and release different DAMP molecules, such as HMGB1 and less consistently HSP90. HMGB1 production and release by OV has been shown to be associated with immune mediated tumor clearance,[48] including in the CNS1 rat GBM model.[21] In vivo, MV+aPD-1 therapy significantly increased the survival of mice bearing orthotopic GL261 GBM compared with single-agent therapies. The constitutive high PD-L1 expression in GL261 cells could represent an important determinant of the efficacy of this immunovirotherapy strategy, even in the context of limited replication of MV strains in murine lines. Ongoing experiments using murine glioma lines (such as the DBT glioma line) with lower PD-L1 expression will allow us to test this hypothesis.

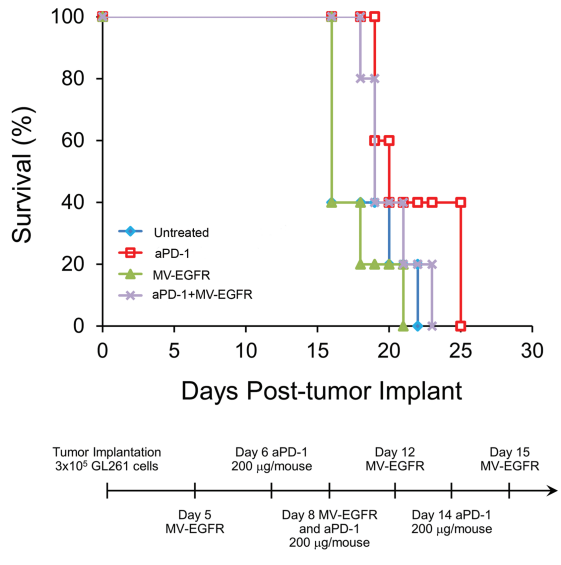

Fig. 5 MV-EGFR+aPD-1 enhanced survival of mice bearing GL261 orthotopic gliomas is dependent on a T-cell mediated response. 3 × 10^5 GL261 glioma cells were orthotopically implanted into athymic nude mice: animals were treated as per the Fig. 3A schema. There was no difference in survival of the MV-EGFR+aPD-1 treated or the aPD-1 monotherapy treated mice compared with untreated animals.

It should be noted that the viral dose of 2×10^5 $TCID_{50}$ used in our experiments is equivalent to approximately 10^8 $TCID_{50}$ in humans (using the FDA commonly recommended brain weight conversion method) and thus it could be directly translatable to a dose level that would be easy to manufacture and administer in a clinical trial. MRI following tail vein administration of CD4 and CD8 antibody conjugated USPIO demonstrated increased proportion of brain infiltrating T cells in mice receiving combination MV-EGFR+aPD-1 therapy compared with all other treatment groups. Further supporting these data, FACS analysis of mouse brains confirmed increased CD8+ T-cell influx into the brains of mice receiving MV-EGFR+aPD-1 therapy compared with the other therapy groups. The requirement of a T-cell mediated response for enhanced survival in the MV-EGFR+aPD-1 therapy group is further supported by the survival analysis of athymic nude mice bearing GL261 orthotopic tumors; there was no significant enhancement of survival for either the MV-EGFR+aPD-1 therapy group or the aPD-1 therapy group compared with the other therapy groups. Of note, aPD-1 does not affect MV replication in infected GBM cells (Supplementary Fig. 3).

In *in vitro* experiments, we demonstrated that MV infection of murine GL261 cells evoked a microglial pro-migratory response in transwell assays. Additionally, qRT-PCR for pro-inflammatory cytokine genes showed that MV infection of GBM cells evoked a pro-inflammatory response from BV2 microglia in coculture. The limited MV-EGFR replication in the GL261 model resulted in a self-limited surge of inflammatory phagocytic cells at 24 hours following viral administration, and thus it does not allow us to conclusively address the role of macrophages in our MV/aPD-1 therapy model. The loss of antitumor activity of this combination regimen in an immunocompromised nude mouse GL261 model (which still has macrophages),[49] however, suggests that macrophages are unlikely to represent a major determinant of the observed antitumor response in this model.

Similar to our results indicating the requirement of a T-cell mediated response for enhanced survival for MV+aPD-1 therapy of GL261 GBM, Rajani et al[43] combined Reovirus+aPD-1 for the treatment of B16 melanoma and found that a CD8+ T-cell mediated response was in part required for the observed enhanced therapeutic efficacy. Additionally, Cockle et al[50] reported on an immunotherapy approach using vaccination with vesicular stomatitis virus (VSV) constructs expressing glioma antigens +aPD-1 therapy for treatment of GL261 gliomas; the observed efficacy in the combination VSV+aPD-1 treatment group was found to be mediated by an IFN-γ driven Th1 response.

This manuscript is the first report demonstrating that combining the activity of oncolytic virotherapy (using a retargeted MV) with aPD-1 blockade results in significant enhancement of survival in a syngeneic orthotopic GBM model. Despite limited MV replication in the GL261 cells, we demonstrated that MV therapy can stimulate a self-limited pro-inflammatory response, which could be effectively augmented by aPD-1 therapy in vivo, resulting in significantly increased animal cure rate via a CD8+ T cell mechanism. While additional mechanistic studies are ongoing, we believe these data support the potential of clinical strategies combining oncolytic virotherapy with aPD-1 therapy for GBM treatment.

Supplementary Material

Supplementary material is available at *Neuro-Oncology* online.

Funding

This work was supported by NIH R01 CA154348, R21 CA186976-1, Mayo Clinic Brain Spore P50 CA10896 and NIH T32 CA108961.

Acknowledgments

We thank the laboratories of Jonathan Godbout, Balveen Kaur, and Susheela Tridandapani at The Ohio State University for their generous gifts of cell lines used in experiments for this report.

Conflict of interest statement. The authors have nothing to declare.

References

1. Johnson DR, Galanis E. Medical management of high-grade astrocytoma: current and emerging therapies. *Semin Oncol* 2014;41:511–522.
2. Allen C, Opyrchal M, Aderca I, et al. Oncolytic measles virus strains have significant antitumor activity against glioma stem cells. *Gene Ther* 2013;20:444–449.
3. Allen C, Paraskevakou G, Iankov I, et al. Interleukin-13 displaying retargeted oncolytic measles virus strains have significant activity against gliomas with improved specificity. *Mol Ther* 2008;16:1556–1564.
4. Allen C, Vongpunsawad S, Nakamura T, et al. Retargeted oncolytic measles strains entering via the EGFRvIII receptor maintain significant antitumor activity against gliomas with increased tumor specificity. *Cancer Res* 2006;66:11840–11850.
5. Opyrchal M, Allen C, Iankov I, et al. Effective radiovirotherapy for malignant gliomas by using oncolytic measles virus strains encoding the sodium iodide symporter (MV-NIS). *Hum Gene Ther* 2012;23:419–427.
6. Phuong LK, Allen C, Peng KW, et al. Use of a vaccine strain of measles virus genetically engineered to produce carcinoembryonic antigen as a novel therapeutic agent against glioblastoma multiforme. *Cancer Res* 2003;63:2462–2469.
7. Paraskevakou G, Allen C, Nakamura T, et al. Epidermal growth factor receptor (EGFR)-retargeted measles virus strains effectively target EGFR- or EGFRvIII expressing gliomas. *Mol Ther* 2007;15:677–686.
8. Ulasov IV, Tyler MA, Zheng S, et al. CD46 represents a target for adenoviral gene therapy of malignant glioma. *Hum Gene Ther* 2006;17:556–564.
9. Dorig RE, Marcil A, Chopra A, et al. The human CD46 molecule is a receptor for measles virus (Edmonston strain). *Cell* 1993;75:295–305.
10. Tatsuo H, Ono N, Tanaka K, et al. SLAM (CDw150) is a cellular receptor for measles virus. *Nature* 2000;406:893–897.
11. Muhlebach MD, Mateo M, Sinn PL, et al. Adherens junction protein nectin-4 is the epithelial receptor for measles virus. *Nature* 2011;480:530–533.

12. Derycke MS, Pambuccian SE, Gilks CB, et al. Nectin 4 overexpression in ovarian cancer tissues and serum: potential role as a serum biomarker. *Am J Clin Pathol* 2010;134:835–845.
13. Fabre-Lafay S, Garrido-Urbani S, Reymond N, et al. Nectin-4, a new serological breast cancer marker, is a substrate for tumor necrosis factor-alpha-converting enzyme (TACE)/ADAM-17. *J Biol Chem* 2005;280:19543–19550.
14. Takano A, Ishikawa N, Nishino R, et al. Identification of nectin-4 oncoprotein as a diagnostic and therapeutic target for lung cancer. *Cancer Res* 2009;69:6694–6703.
15. Geekiyanage H, Galanis E. Mir-31 and miR-128 regulates poliovirus receptor-related 4 (PVRL4) mediated measles virus infectivity in tumors. *Mol Oncol* 2016. http://dx.doi.org/10.1016/j.molonc.2016.07.007
16. Nduom EK, Wei J, Yaghi NK, et al. PD-L1 expression and prognostic impact in glioblastoma. *Neuro Oncol* 2016;18:195–205.
17. Bloch O, Crane CA, Kaur R, et al. Gliomas promote immunosuppression through induction of B7-H1 expression in tumor-associated macrophages. *Clin Cancer Res* 2013;19:3165–3175.
18. Fecci PE, Mitchell DA, Whitesides JF, et al. Increased regulatory T-cell fraction amidst a diminished CD4 compartment explains cellular immune defects in patients with malignant glioma. *Cancer Res* 2006;66:3294–3302.
19. da Fonseca AC, Badie B. Microglia and macrophages in malignant gliomas: recent discoveries and implications for promising therapies. *Clin Dev Immunol* 2013;2013:264124.
20. Gustafson MP, Lin Y, New KC, et al. Systemic immune suppression in glioblastoma: the interplay between CD14+HLA-DRlo/neg monocytes, tumor factors, and dexamethasone. *Neuro Oncol* 2010;12:631–644.
21. Curtin JF, Liu N, Candolfi M, et al. HMGB1 mediates endogenous TLR2 activation and brain tumor regression. *PLoS Med* 2009;6:e10.
22. Donnelly OG, Errington-Mais F, Steele L, et al. Measles virus causes immunogenic cell death in human melanoma. *Gene Ther* 2013;20:7–15.
23. Gauvrit A, Brandler S, Sapede-Peroz C, et al. Measles virus induces oncolysis of mesothelioma cells and allows dendritic cells to cross-prime tumor-specific CD8 response. *Cancer Res* 2008;68:4882–4892.
24. Huang B, Sikorski R, Kirn DH, et al. Synergistic anti-tumor effects between oncolytic vaccinia virus and paclitaxel are mediated by the IFN response and HMGB1. *Gene Ther* 2011;18:164–172.
25. Liikanen I, Ahtiainen L, Hirvinen ML, et al. Oncolytic adenovirus with temozolomide induces autophagy and antitumor immune responses in cancer patients. *Mol Ther* 2013;21:1212–1223.
26. Miyamoto S, Inoue H, Nakamura T, et al. Coxsackievirus B3 is an oncolytic virus with immunostimulatory properties that is active against lung adenocarcinoma. *Cancer Res* 2012;72:2609–2621.
27. Bartlett DL, Liu Z, Sathaiah M, et al. Oncolytic viruses as therapeutic cancer vaccines. *Mol Cancer* 2013;12:103.
28. Galanis E, Atherton PJ, Maurer MJ, et al. Oncolytic measles virus expressing the sodium iodide symporter to treat drug-resistant ovarian cancer. *Cancer Res* 2015;75:22–30.
29. Carlson BL, Pokorny JL, Schroeder MA, et al. Establishment, maintenance and *in vitro* and *in vivo* applications of primary human glioblastoma multiforme (GBM) xenograft models for translational biology studies and drug discovery. *Curr Protoc Pharmacol* 2011;Chapter 14:Unit 14 16.
30. Dingli D, Peng KW, Harvey ME, et al. Image-guided radiovirotherapy for multiple myeloma using a recombinant measles virus expressing the thyroidal sodium iodide symporter. *Blood* 2004;103:1641–1646.
31. Duprex WP, McQuaid S, Hangartner L, et al. Observation of measles virus cell-to-cell spread in astrocytoma cells by using a green fluorescent protein-expressing recombinant virus. *J Virol* 1999;73:9568–9575.
32. Meisen WH, Wohleb ES, Jaime-Ramirez AC, et al. The Impact of Macrophage- and Microglia-Secreted TNFalpha on Oncolytic HSV-1 Therapy in the Glioblastoma Tumor Microenvironment. *Clin Cancer Res* 2015;21:3274–3285.
33. Pirko I, Johnson A, Ciric B, et al. In vivo magnetic resonance imaging of immune cells in the central nervous system with superparamagnetic antibodies. *Faseb J* 2004;18:179–182.
34. Takeuchi K, Kadota SI, Takeda M, et al. Measles virus V protein blocks interferon (IFN)-alpha/beta but not IFN-gamma signaling by inhibiting STAT1 and STAT2 phosphorylation. *FEBS Lett* 2003;545:177–182.
35. Kim TG, Kim CH, Park JS, et al. Immunological factors relating to the antitumor effect of temozolomide chemoimmunotherapy in a murine glioma model. *Clin Vaccine Immunol* 2010;17:143–153.
36. Niewiesk S, Schneider J, Ohnimus H, et al. CD46 expression does not overcome the intracellular block of measles virus replication in transgenic rats. *J Virol* 1997;71:7969–7973.
37. Vincent S, Tigaud I, Schneider H, et al. Restriction of measles virus RNA synthesis by a mouse host cell line: trans-complementation by polymerase components or a human cellular factor(s). *J Virol* 2002;76:6121–6130.
38. Yang HW, Lu YJ, Lin KJ, et al. EGRF conjugated PEGylated nanographene oxide for targeted chemotherapy and photothermal therapy. *Biomaterials* 2013;34:7204–7214.
39. Ginhoux F, Lim S, Hoeffel G, et al. Origin and differentiation of microglia. *Front Cell Neurosci* 2013;7:45.
40. Stansley B, Post J, Hensley K. A comparative review of cell culture systems for the study of microglial biology in Alzheimer's disease. *J Neuroinflammation* 2012;9:115.
41. Henn A, Lund S, Hedtjarn M, et al. The suitability of BV2 cells as alternative model system for primary microglia cultures or for animal experiments examining brain inflammation. *Altex* 2009;26:83–94.
42. Fulci G, Breymann L, Gianni D, et al. Cyclophosphamide enhances glioma virotherapy by inhibiting innate immune responses. *Proc Natl Acad Sci U S A* 2006;103:12873–12878.
43. Rajani K, Parrish C, Kottke T, et al. Combination Therapy With Reovirus and Anti–PD-1 Blockade Controls Tumor Growth Through Innate and Adaptive Immune Responses. *Mol Ther* 2015.
44. Engeland CE, Grossardt C, Veinalde R, et al. CTLA-4 and PD-L1 checkpoint blockade enhances oncolytic measles virus therapy. *Mol Ther* 2014;22:1949–1959.
45. Kaufmann JK, Chiocca EA. Glioma virus therapies between bench and bedside. *Neuro Oncol* 2014;16:334–351.
46. Thomas AA, Brennan CW, DeAngelis LM, et al. Emerging therapies for glioblastoma. *JAMA Neurol* 2014;71:1437–1444.
47. Zeng J, See AP, Phallen J, et al. Anti–PD-1 blockade and stereotactic radiation produce long-term survival in mice with intracranial gliomas. *Int J Radiat Oncol Biol Phys* 2013;86:343–349.
48. Kang R, Zhang Q, Zeh HJ, et al. HMGB1 in cancer: good, bad, or both? *Clin Cancer Res* 2013;19:4046–4057.
49. Budzynski W, Radzikowski C. Cytotoxic cells in immunodeficient athymic mice. *Immunopharmacol Immunotoxicol* 1994;16:319–346.
50. Cockle JV, Rajani K, Zaidi S, et al. Combination viroimmunotherapy with checkpoint inhibition to treat glioma, based on location-specific tumor profiling. *Neuro Oncol* 2016;18:518–527.